Decoupling the influences of chiral damping and Dzyaloshinskii-Moriya interaction in chiral magnetic domain walls

Collins Ashu Akosa,[1,2,3,*] Gen Tatara,[2] Aurélien Manchon,[4] and Masahito Mochizuki[1]
[1]*Department of Applied Physics, Waseda University, Okubo, Shinjuku-ku, Tokyo 169-8555, Japan*
[2]*RIKEN Center for Emergent Matter Science (CEMS), Wako, Saitama 351-0198, Japan*
[3]*Department of Theoretical and Applied Physics, African University of Science and Technology (AUST), Galadimawa, Abuja F.C.T 900107, Nigeria*
[4]*Aix-Marseille Université, CNRS, CINaM, Marseille, France*

(Received 7 May 2024; revised 28 June 2024; accepted 28 June 2024; published 16 July 2024)

We revisit the nature and impact of both the chiral damping (CD) and Dzyaloshinskii-Moriya interaction (DMI) in uniaxial chiral ferromagnetic nanowires with broken inversion symmetry. We propose that CD, akin to its chiral energy counterpart (DMI), can be described in terms of the Lifshitz invariants permissible by the underlying symmetry of the system. This representation offers a clearer foundation for integrating CD into the dynamics of various chiral magnetic textures. We theoretically investigate the current-induced motion of chiral domain walls (DWs), driven by both spin-transfer torque and the spin Hall effect in the presence of CD. We demonstrate that it is possible to unambiguously separate the influence of CD from that of DMI by analyzing the current-induced dynamics. In particular, below the Walker breakdown (WB), the DMI does not affect the DW velocity, whereas increases in the strength of CD result in a decrease in the DW velocity. Moreover, for the spin-orbit torque driven motion, while the DMI enhances both the WB current density and the maximum attainable velocity below the WB, the CD only enhances the WB without affecting the maximum attainable velocity below the WB. Our findings open up intriguing opportunities for exploitation in exotic magnetic textures.

DOI: 10.1103/PhysRevB.110.024420

I. INTRODUCTION

Nature often produces swirling or twisting objects with a preferred rotation sense, which affects their energy, making it lower for one rotation sense than the other. In condensed-matter systems, such a preference is governed by terms containing the Lifshitz invariant [1,2]

$$\mathcal{L}_{\mu\nu}^{(\gamma)} = m_\mu \frac{\partial m_\nu}{\partial x_\gamma} - m_\nu \frac{\partial m_\mu}{\partial x_\gamma}, \quad (1)$$

in the energy functional, where m is a unit vector in the direction of the local magnetization. The invariant given by Eq. (1) is inherent in systems with intrinsic and/or induced chirality. Magnets with broken inversion symmetry is a typical example of the latter, where spin-orbit interaction (SOI) in the crystal with inversion-broken symmetry mediates an asymmetric exchange interaction called the Dzyaloshinskii-Moriya interaction (DMI). This interaction is a central mechanism for stabilizing the spatially modulated structures of local magnetic moments and even determines their rotation sense [3–5]. It turns out that there exists a dissipative counterpart of DMI, called chiral damping (CD). Despite being demonstrated experimentally [6–8] and supported by various theoretical studies [9–12], the impact of CD on the dynamics of domain walls (DWs) and skyrmions has been challenging to determine unambiguously partly due to the difficulty of distinguishing its effect from that of DMI. Therefore, it is necessary to explore different approaches and techniques to determine whether the chirality-induced asymmetry in the current and field-driven behavior of magnetic textures is predominantly linked to CD or DMI.

Furthermore, it is important to note that magnetization dissipation not only significantly influences how magnets respond to external stimuli but also plays a fundamental role in understanding magnetic phenomena like switching, DW dynamics, and spin transport. Although there have been investigations into CD in ferromagnets, spanning from phenomenological descriptions to microscopic models [6–12], existing literature has lacked a systematic examination of CD in exotic systems like ferri- and antiferromagnets. Indeed, damping and spin pumping studies in two-sublattice magnets suggest that the previously overlooked interactions between sublattices have a significant influence on the effective damping [13–15]. It turns out that since the dynamics of itinerant electrons (that mediate damping in metallic systems) is distinct from those of the local magnetization (that controls the magnetostatics), one expects an asymmetry in the sublattice's effective damping via the CD contribution even in the case of an antiferromagnet with equivalent sublattices.

However, the phenomenological manner in which CD has been incorporated presents challenges in extending it to these exotic systems. This sets the groundwork for the present study.

*Contact author: collins.akosa@aoni.waseda.jp

The outstanding question raised for chiral magnetic textures is whether one can unambiguously separate the effect of CD from the effect of DMI. Indeed, up until now, there is no clear consensus on isolating the impact of CD on the dynamics of magnetic texture from that of the DMI [16–19]. This can be attributed partly to the fact that a microscopic derivation of the CD, which was originally introduced phenomenologically, involves many free parameters. Moreover, there is no experimental method to verify or measure the effect of CD directly. It is thus expected that the systematic treatment and a closer examination of the nature of CD in exotic systems would provide a guide and open new avenues to investigate and eventually unambiguously isolate the effect of CD from DMI.

In this study, we use heuristic symmetry considerations, backed by recent studies, to introduce a more elucidating description of CD and establish a comprehensive framework for analyzing the distinct effects of CD and DMI in chiral magnetic systems. We suggest that CD, just as its chiral energy counterpart (DMI) can be described in terms of the Lifshitz invariants permissible by the underlying symmetry of the system. We theoretically investigate the current-induced motion of chiral DWs, driven by both spin-transfer torque and the spin Hall effect in the presence of CD. We demonstrate that it is possible to unambiguously separate the influence of CD from that of DMI by analyzing the current-induced dynamics. Our findings open up intriguing opportunities for exploitation in exotic magnetic textures.

II. THEORETICAL MODEL

The damping tensor $\boldsymbol{\alpha}(\mathbf{r}, t)$, similar to the free-energy density of magnetic systems, can be expressed in terms of the spatial magnetization gradient, with an expansion up to first order as [20]

$$\alpha_{\mu\nu} = \alpha^{(0)}_{\mu\nu} + \alpha^{(1)}_{\mu\nu\gamma\rho} m_\gamma m_\rho + \alpha^{(2)}_{\mu\nu\gamma\rho\lambda} m_\gamma \partial_\lambda m_\rho, \tag{2}$$

where the tensors $\alpha^{(0)}_{\mu\nu}$, $\alpha^{(1)}_{\mu\nu\gamma\rho}$, and $\alpha^{(2)}_{\mu\nu\gamma\rho\lambda}$ are invariant under the point group of the system in accordance to Neumann's principle [21]. $\alpha^{(2)}_{\mu\nu\gamma\rho\lambda}$ is the CD term that only appears in chiral magnets characterized by broken spatial inversion symmetry. This simple heuristic symmetry argument suggests that just like the DMI (chirality-dependent energy), the CD (chirality-dependent dissipation) can be described by the Lifshitz invariants in Eq. (1) in accordance with previous studies [6,8–12,20,22,23]. It is well known that magnetic damping affects magnetization dynamics and not magnetostatics, whereas the DMI has been shown to influence both the static and dynamics of magnetization.

Moreover, since it has been established that the DMI and CD are intricately linked to the nature of the SOI [12,18] in the system, in what follows, we consider, without loss of generality, the interplay between Rashba and Dresselhaus SOI, inherent in systems with interfacial and bulk inversion symmetry breaking [24,25], respectively. We provide such comprehensive treatment to allow for extension to other systems such as magnetic skyrmions, hopfions, and antiferromagnets. Additionally, we provide a qualitative analogy between chirality-dependent energy and chirality-dependent dissipation, which are intimately connected by virtue of symmetry and microscopic origin—SOI.

Let us first consider a one-dimensional magnetic texture varying along the x-direction such as a DW. The chiral energy density reads

$$\mathcal{E}_{\rm c} = D_{\rm R}\mathcal{L}^{(x)}_{zx} + D_{\rm D}\mathcal{L}^{(x)}_{zy}, \tag{3}$$

where $D_{\rm R(D)}$ denotes the Dzyaloshinskii-Moriya constant specific to the material [23]. To derive a similar expression for chiral dissipation, we start by acknowledging that the CD described in Eq. (2) generally takes the form of a second-rank tensor. Nonetheless, in an isotropic scenario (i.e., $\alpha_{\mu\nu} \sim \alpha\delta_{\mu\nu}$), the chiral dissipation can be expressed in terms of the Lifshitz invariants in Eq. (1) using Eq. (2) as [26,27]

$$\alpha_{\rm c}(x) = \Lambda_{\rm R}\mathcal{L}^{(x)}_{zx} + \Lambda_{\rm D}\mathcal{L}^{(x)}_{zy}. \tag{4}$$

Here, $\Lambda_{\rm R(D)}$ represents material constants with dimensions of length, which are proportional to the strength of Rashba (Dresselhaus) SOI. Obviously, a major challenge is the design of experiments to measure $\Lambda_{\rm R(D)}$ which is outside of the scope of this work. However, we suggest a setup and possible material realization in which one could acquire a qualitative assessment of the latter. Moreover, experimental evidence has shown that by applying an external gate voltage, it is possible to alter the inversion symmetry of a crystalline lattice structure [28,29]. This presents an avenue to adjust the strength of the CD in materials, whether they exhibit bulk inversion symmetry breaking or interfacial inversion symmetry breaking. Quasi-two-dimensional material systems with interfacial symmetry breaking such as $\mathrm{LaAl0_3/SrTiO_3}$, $\mathrm{SrIrO_3/SrRuO_3}$, or $\mathrm{SrRuO_3/SrTiO_3}$ are promising materials of interest. Another avenue worth exploring involves systems exhibiting B20 symmetry like MnSi and FeCoSi, as well as strained zinc-blende structures like MnNiSb [30], which exhibit bulk inversion symmetry breaking. Before we proceed, it is necessary to address some key points regarding the proportionality constant associated with chirality-dependent dissipation. First, it is important to acknowledge that $\Lambda_{\rm R(D)}$ varies in proportion to the strength of the SOI [8,12] just as the DMI [18]. Second, one would anticipate the sign of $\Lambda_{\rm R(D)}$ to be opposite to the sign of $D_{\rm R(D)}$ because a decrease in magnetic energy due to the DMI should correspond to an increase in magnetic damping. This aligns with prior studies indicating that the combined impact of spin mixing and momentum scattering around the DW leads to an enhancement of the damping [31–33]. However, it is worth noting that the possibility of the influence of Hund's rule coupling in some heavy metals and inhomogeneity-induced anisotropic effects in real materials cannot be ruled out. In such cases, it is plausible for $D_{\rm R(D)}$ and $\Lambda_{\rm R(D)}$ to have the same sign, potentially resulting in an overall decrease in the effective damping. This scenario is particularly relevant in metallic systems where conduction electrons play a dominant role in angular momentum transfer. In such systems, the induced chirality in these electrons may inherit certain anisotropic properties due to intrinsic material inhomogeneities.

To elucidate the influence of CD on the dynamics of DWs, we make two specific assumptions. First, we presume that strength of the CD can be tailored separately from the DMI. This assumption is inferred from the understanding that damping in metallic systems is mediated by the spins of conduction electrons [34–38], whose dynamics is distinct from that of the local magnetizations interacting through the DMI. As a result, it should be feasible to manipulate the CD without necessarily impacting the DMI. Essentially, while DMI governs both the dynamic and static characteristics of magnetic textures, CD solely affects their dynamics. Alternatively, another plausible perspective arises from the notion that both CD and DMI can be tuned simultaneously and coherently. This is because they stem from a shared microscopic mechanism—the SOI with broken inversion symmetry—and both are linear in the strength of the SOI. Hence, to minimize the number of free parameters, we introduce the following correlation:

$$\Lambda_{\mathrm{R(D)}} = \chi^{\mathrm{cd}}_{\mathrm{R(D)}} D_{\mathrm{R(D)}}. \tag{5}$$

In this manner, the DMI and CD are treated on equal footing, with $\chi^{\mathrm{cd}}_{\mathrm{R(D)}}$ representing a material-specific scaling factor.

Finally, it is important to highlight that a recent study indicates that the CD term similar to the form and symmetry in Eq. (4) emerges from the interplay of broken inversion symmetry, SOI, and magnetic texture through multibody scattering processes [23]. Furthermore, since dissipation does not significantly affect magnetostatics, the stabilizable magnetic texture in the system is not critically influenced by the nature of CD. In the subsequent section, we explore the effects of CD on the dynamics of DWs driven by electric currents via both the spin-transfer torque and spin-orbit torque mechanisms.

III. CURRENT-DRIVEN DW DYNAMICS

In this section, we examine the current-induced dynamics of a chiral magnetic DW subjected to a nonlocal CD. This is modeled via a modified Landau-Lifshitz-Gilbert equation, given as

$$\begin{aligned}\partial_t \mathbf{m} = -\gamma \mathbf{m} \times \mathbf{H}_{\mathrm{eff}} + \alpha_{\mathrm{eff}} \mathbf{m} \times \partial_t \mathbf{m} - b_J \partial_x \mathbf{m} \\ + \beta b_J \mathbf{m} \times \partial_x \mathbf{m} + \gamma H_{\mathrm{sh}} \mathbf{m} \times (\mathbf{y} \times \mathbf{m}),\end{aligned} \tag{6}$$

where $\mathbf{H}_{\mathrm{eff}}$ is the effective field that includes anisotropy, exchange, DMI, and demagnetizing fields.

$$\alpha_{\mathrm{eff}} = \alpha_0 + \alpha_{\mathrm{c}}(x) \tag{7}$$

is the effective damping that consists of the constant Gilbert damping constant α_0 and the nonlocal CD contribution α_{c} given by Eq. (4). The third and fourth terms on the right-hand side of Eq. (6) are the adiabatic and nonadiabatic spin-transfer torque terms, where $b_{\mathrm{J}} = u_B P j_e/(eM_s)$ is the magnitude of the adiabatic torque, P is the spin polarization, j_e is the current density flowing through the ferromagnetic layer, e is the magnitude of electron's charge, M_s is the saturation magnetization, μ_B is the Bohr magneton, and β is the conventional nonadiabaticity parameter. The last term in Eq. (6) is the contribution from spin-orbit torque arising from spin Hall effect with $H_{\mathrm{sh}} = \hbar\theta_{\mathrm{sh}} j_e/(et_F\mu_0 M_s)$, where $\hbar$ is the reduced Planck's constant, θ_{sh} is the spin Hall angle for current polarization along the y-direction, μ_0 is the vacuum permeability, and t_F is the magnetic film thickness. For the remainder of this article, we simplify our focus to a Rashba system characterized by the breaking of interfacial inversion symmetry along the z-direction. This results can be readily extended to the case of systems with bulk inversion symmetry breaking in which the Desselhauss SOI is dominant. Furthermore, we consider, without loss of generality, the analytical ansatz for a one-dimensional case DW along the x-direction parameterized by its collective coordinates for the wall center X and tilt angle ϕ:

$$\mathbf{m}(x, t) = (\cos\phi \sin\theta, \sin\phi \sin\theta, \cos\theta) \tag{8}$$

and

$$\theta = 2\tan^{-1}\{\exp[s(x - X)/\lambda]\}, \tag{9}$$

where λ is the DW width, and $s = \pm 1$ describes the DW chirality ($\uparrow\downarrow$ or $\downarrow\uparrow$, respectively). Integrating of Eq. (6) over this DW profile and following standard procedure based on Thiele's formalism of rigid structure [39], we obtain the following set of equations:

$$\frac{s\partial_t X}{\lambda} - \bar{\alpha}_{\mathrm{eff}}\partial_t\phi = \frac{sb_J}{\lambda} + \gamma H_{xy}\sin 2\phi - \frac{s\pi}{2}\gamma H_{\mathrm{dm}}\sin\phi \tag{10a}$$

and

$$\partial_t\phi + \bar{\alpha}_{\mathrm{eff}}\frac{s\partial_t X}{\lambda} = \frac{s\beta b_J}{\lambda} + \frac{\pi}{2}\gamma H_{\mathrm{sh}}\cos\phi, \tag{10b}$$

where $H_{\mathrm{dm}} = D_R/\mu_0 M_s\lambda$ is the effective field due to DMI and $H_{xy} = (N_y - N_x)M_s/2$ is the in-plane demagnetizing field. $\bar{\alpha}_{\mathrm{eff}}$ represents the total effective damping such that $\bar{\alpha}_{\mathrm{eff}} \equiv \alpha_0 + \bar{\alpha}_c$, and contains both the contribution from Gilbert damping α_0 and the average nonlocal CD contribution $\bar{\alpha}_c$ calculated as $\bar{\alpha}_c \equiv \int_{-\infty}^{+\infty} dx\, \alpha_{\mathrm{c}}(x)\, \partial_x\mathbf{m}\cdot\partial_x\mathbf{m}/\int_{-\infty}^{+\infty} dx\, \partial_x\mathbf{m}\cdot\partial_x\mathbf{m}$ given as

$$\bar{\alpha}_c = \frac{s\pi\Lambda_{\mathrm{R}}}{4\lambda}\cos\phi. \tag{11}$$

Notice that the spatial average of the CD contribution is not a constant and depends on the DW tilt angle ϕ, which determines the chirality of the DW, hence its name. Moreover, in considering the ansatz of the DW profile above, we have neglected the effect of DW canting due to the application of in-plane magnetic field [40,41], since such canting does not affect the physics under consideration. The solution of Eqs. (10a) and (10b) yield

$$\begin{aligned}\frac{s\partial_\tau X}{\lambda} = (1 + \beta\bar{\alpha}_{\mathrm{eff}})\frac{sb_J}{\lambda\gamma} + H_{xy}\sin 2\phi \\ + \bar{\alpha}_{\mathrm{eff}}\frac{\pi}{2}H_{\mathrm{sh}}\cos\phi - \frac{s\pi}{2}H^{\mathrm{R}}_{\mathrm{dm}}\sin\phi\end{aligned} \tag{12a}$$

and

$$\begin{aligned}\partial_\tau\phi = (\beta - \bar{\alpha}_{\mathrm{eff}})\frac{sb_J}{\lambda\gamma} + \frac{\pi}{2}H_{\mathrm{sh}}\cos\phi \\ - \bar{\alpha}_{\mathrm{eff}}H_{xy}\sin 2\phi + s\bar{\alpha}_{\mathrm{eff}}\frac{\pi}{2}H^{\mathrm{R}}_{\mathrm{dm}}\sin\phi,\end{aligned} \tag{12b}$$

where $\tau = \gamma t/(1 + \bar{\alpha}^2_{\mathrm{eff}})$. The direct implication is that depending on the type of application, one can smartly tune (reduce or enhance) the damping parameter of the material via smart material engineering. As a result the so-called Walker breakdown (WB) field [42] can be tuned accordingly since it is proportional to the strength of the effective damping. Below the WB, the DW tilt angle is considered to be on

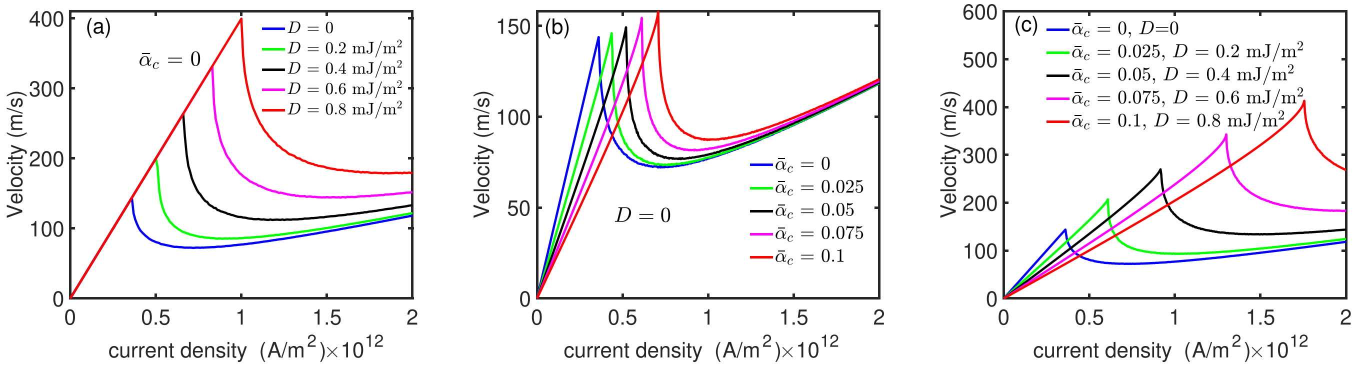

FIG. 1. The dependence of DW velocity on the current density in the presence of DMI and/or CD driven by spin-transfer torque. (a) In the absence of chiral contribution to the damping ($\bar{\alpha}_c = 0$), both the $j_e^{\rm WB}$ and $v_{\rm max}^{\rm WB}$ increase with an increase in the strength of DMI. (b) For a fixed DMI strength ($D = 0$), an increase in the strength of CD and thus the effective damping leads to an increase in the $j_e^{\rm WB}$, but only slightly alters $v_{\rm max}^{\rm WB}$. (c) In the scenario where both DMI and CD are present, an increase in the strength of the SOI—and consequently an increase in both the strength of DMI and CD—results in an increase in both the $v_{\rm max}^{\rm WB}$ and the $j_e^{\rm WB}$.

average stationary, i.e., $\partial_t \phi = 0$, we obtain the expression of the velocity of the DW as

$$\partial_t X = \frac{1}{\bar{\alpha}_{\rm eff}}\left(\beta b_J + \frac{s\pi}{2}\lambda\gamma H_{\rm sh}\cos\phi\right). \tag{13}$$

We can immediately see that one can drive the DW much faster or slower, depending on the relative contribution from the CD. Our findings does not only corroborate previous studies on the subject matter [6,8–12,20,22,23] but also (i) serves as a transparent and more general basis for integrating CD in magnetic systems for arbitrary type of SOI and underlying symmetries, and (ii) provides a solid background and framework for exploring this phenomenon in more exotic systems, such as two-sublattice antiferromagnets, skyrmions, and hopfions.

IV. NUMERICAL RESULTS

To gain further insight into the interplay between CD and DMI on the current-induced dynamics of chiral DWs, we consider the numerical integration of the coupled equations given by Eqs. (12a) and (12b). For the simulations, we chose typical micromagnetic parameters, namely $A = 12.5$ pJ/m, $\mu_0 M_s =$ 1 T, and $K = 0.495$ MJ/m^3, which give rise to a DW width of $\lambda \approx \sqrt{A/(K - \mu_0 M_s^2/2)} = 10$ nm. Furthermore, a Rashba SOI strength of 1.67×10^{-11}eV m translates to a characteristic length scale of $\Lambda_{\rm R} = 0.25$ nm [43] and corresponds to a CD strength of $\bar{\alpha}_c = 0.02$. Moreover, for all of our simulations, we used $\gamma = 2.21 \times 10^5$ m/(A.s), $\alpha_0 = 0.1$, $\beta = 0.8$, $P = 0.69$, $\theta_{\rm sh} = 0.15$, $t_F = 2$ nm, and demagnetizing factors of $N_y = 0.0723$, $N_x = 0$, and $N_z = 0.9277$, which depends on the geometry of the system [44–46]. These values corresponds to an in-plane demagnetizing field strength of $\mu_0 H_{xy} \approx$ 10 mT, and a WB field strength of $\mu_0 H_{\rm wb}^0 \approx 1$ mT (in the absence of both DMI and CD).

It is important to note that the chirality of the DW is determined by the sign of the DMI, meaning that we establish the chirality corresponding to the lowest energy state. First, we present a control simulation in which the dependence of DW velocity on current density resulting from the conventional spin-transfer torque is probed in the absence of CD for different strengths of the DMI as depicted in Fig. 1(a). The latter shows that the effect of DMI is threefold: (i) fixes the DW chirality, (ii) enhances the WB current density ($j_e^{\rm WB}$), and (iii) increases the maximum attainable DW velocity below WB ($v_{\rm max}^{\rm WB}$), consistent with previous studies [46]. It is noteworthy that at a fixed current density below $j_e^{\rm WB}$, DMI does not affect the DW velocity. However, above $j_e^{\rm WB}$, an increase in the strength of DMI leads to an increase in the DW velocity. Next, we re-examine the DW velocity versus current density behavior, this time for different strengths of the CD [12] as shown in Fig. 1(b). We immediately identify two distinctive features between CD and DMI, namely (i) unlike DMI, the CD has a negligible effect on $v_{\rm max}^{\rm WB}$, and (ii) at a fixed current density below $j_e^{\rm WB}$, the DW velocity decreases with an increase in the strength of the CD. Conversely, above $j_e^{\rm WB}$, the opposite trend is observed: the DW velocity increases with an increase in the strength of the CD. This stems from the fact that the CD can be understood as an additional damping [i.e., $\alpha_{\rm eff} = \alpha_0 + \bar{\alpha}_c(\phi)$], and as such, it enhances both the damping and $j_e^{\rm WB}$ [i.e., $j_e^{\rm WB} \propto \alpha_{\rm eff}/(\beta - \alpha_{\rm eff})$]. From Eq. (13), we can infer that $v_{\rm max}^{\rm WB}$ shows a weak dependence on the CD via $\alpha_{\rm eff}$ [i.e., $v_{\rm max}^{\rm WB} \propto 1/(\beta - \alpha_{\rm eff})$]. Moreover, by extracting the values of $v_{\rm max}^{\rm WB}$ and $j_e^{\rm WB}$ for varying strengths of CD and DMI, our findings can be effectively illustrated, as depicted in Fig. 2. This weak enhancement as depicted in Figs. 1(b) and 2(a) is obviously insufficient to physically and/or qualitatively separate the effect DMI from that of CD because the reported change in $v_{\rm max}^{\rm WB}$ are within the typical error bars involved in such measurements.

In Fig. 1(c), we show the dependence of the DW velocity as a function of current density in the system in which DMI and CD are incorporated coherently via Eq. (5). As expected, we observed a simultaneous enhancement of the $j_e^{\rm WB}$ due to a combination of DMI and CD and an enhancement of $v_{\rm max}^{\rm WB}$ predominantly due to DMI. In summary, a key distinguishing feature between CD and the DMI in the current-induced dynamics of chiral DWs driven by spin-transfer torque is their velocity dependence below the WB. Specifically, below the WB, the DMI does not affect the DW velocity, whereas increase in the strength of CD results in a decrease in the DW velocity.

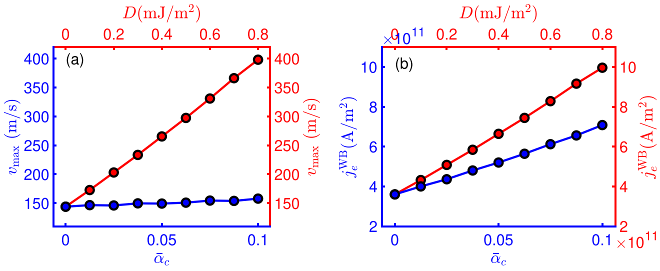

FIG. 2. The dependence of $v_{\max}^{\mathrm{WB}}$ and j_e^{WB} on the strengths of $\bar{\alpha}_c$ (blue) and D (red), driven by spin-transfer torque. (a) For a fixed CD ($\bar{\alpha}_c = 0$), increasing D leads to an increase in $v_{\max}^{\mathrm{WB}}$. Conversely, with a fixed DMI ($D = 0$), increase in $\bar{\alpha}_c$ only slightly modifies $v_{\max}^{\mathrm{WB}}$. (b) With a fixed DMI strength ($D = 0$), increasing $\bar{\alpha}_c$ and thus the effective damping results in an increase in j_e^{WB}. Similarly, when the CD is fixed ($\bar{\alpha}_c = 0$), an increase in D leads to an increase in j_e^{WB}.

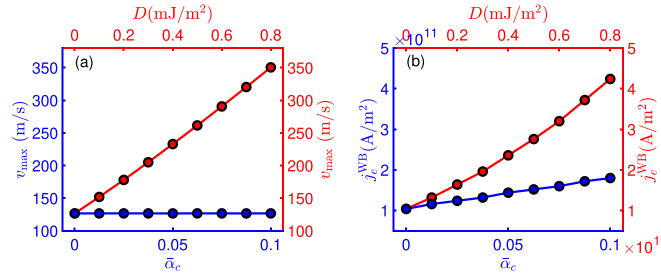

FIG. 4. CD (blue) and DMI (red) dependence of $v_{\max}^{\mathrm{WB}}$ and j_e^{WB} for spin-orbit torque-driven DW dynamics. (a) For a fixed CD ($\bar{\alpha}_c = 0$), increasing D leads to an increase in $v_{\max}^{\mathrm{WB}}$. However, with a fixed DMI ($D = 0$), increase in $\bar{\alpha}_c$ does not affect $v_{\max}^{\mathrm{WB}}$. (b) With a fixed DMI strength ($D = 0$), increasing $\bar{\alpha}_c$ leads to an increase in j_e^{WB}. Similarly, when the CD is fixed ($\bar{\alpha}_c = 0$), an increase in D also results in an increase in j_e^{WB}.

To address the question of whether it is possible to clearly distinguish the influence of the DMI from that of CD, we thoroughly examine the dynamics of the DW driven by spin-orbit torque originating from the spin Hall effect. The DW velocity (c.f. Néel DW, $\phi = 0$) as a function of the current density for various strengths of CD and DMI is summarized in Figs. 3 and 4. Similar to the dynamics driven by spin-transfer torque as presented above, Fig. 3(a) (see also red curves in Fig. 4) demonstrates that in the absence of CD, the dynamics driven by spin-orbit torque for different strengths of the DMI lead to an enhancement in both j_e^{WB} and $v_{\max}^{\mathrm{WB}}$, consistent with Eqs. (12a) and (12b). Moreover, the symmetry of the spin-orbit torque, which is proportional to $\cos\phi$, renders it most effective in driving Néel DWs. Coupled with the influence of the DMI on the tilt angle ϕ of the DW, $v_{\max}^{\mathrm{WB}}$ indeed represents the maximum achievable velocity even beyond the WB limit. Additionally, similar to the scenario with spin-transfer torque, below the WB, the DMI does not influence the DW velocity, whereas an increase in the strength of CD leads to a decrease in the DW velocity.

Another notable finding in this study is depicted in Fig. 3(b) (see also blue curves in Fig. 4), where we identify another distinctive feature between CD and the DMI: unlike the DMI, CD does not impact $v_{\max}^{\mathrm{WB}}$. Specifically, for a fixed strength of the DMI ($D = 0$, for simplicity), varying strengths of the CD only lead to an enhancement of j_e^{WB} while keeping $v_{\max}^{\mathrm{WB}}$ unchanged. This not only facilitates the unambiguous separation of the effects of DMI from CD in chiral magnets but also provides a method through which one can estimate the contribution of CD in the system. In particular, by driving a chiral Néel DW using spin-orbit torque generated from the spin Hall effect at various gate-tuned strengths of the SOI [47–49], one can measure the change in the WB current density Δj_e^{WB}. From this measurement, the strength of the CD in the system can be estimated as

$$\bar{\alpha}_c \approx \frac{\Delta j_e^{\mathrm{WB}}}{j_e^{\mathrm{WB}^0}} \alpha_0, \tag{14}$$

where $j_e^{\mathrm{WB}^0}$ is the WB current density at zero voltage. Moreover, having knowledge of the value $\bar{\alpha}_c$ provides us with

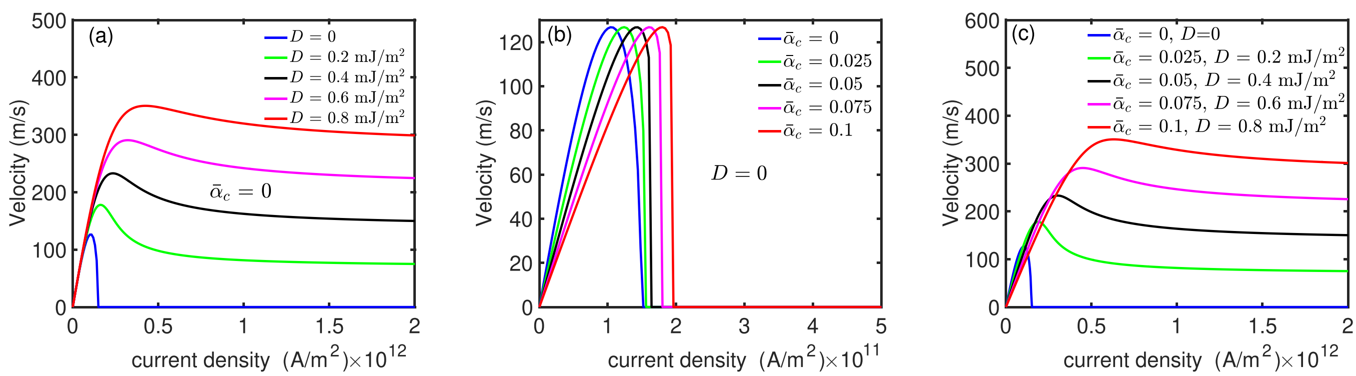

FIG. 3. The dependence of DW velocity on the current density in the presence of DMI and/or CD driven by spin-orbit torque. (a) In the absence of chiral contribution to the damping ($\bar{\alpha}_c = 0$), both the j_e^{WB} and $v_{\max}^{\mathrm{WB}}$ increase with an increase in the strength of DMI. (b) For a fixed DMI strength ($D = 0$), an increase in the strength of CD and thus the effective damping enhances the j_e^{WB} but does not alter $v_{\max}^{\mathrm{WB}}$. Above the WB, both the CD and the spin-orbit torque vanish due to their inherent ϕ-dependence (i.e., $\propto \cos\phi$). (c) In the presence of both DMI and CD, an increase in the strength of the SOI—and consequently an increase in both the strength of DMI and CD—results in an increase in both the $v_{\max}^{\mathrm{WB}}$ and j_e^{WB}. Above the WB, a nonzero DMI induces a finite DW tilt ϕ, resulting in both CD and spin-orbit torque remaining finite and producing a nonzero DW velocity.

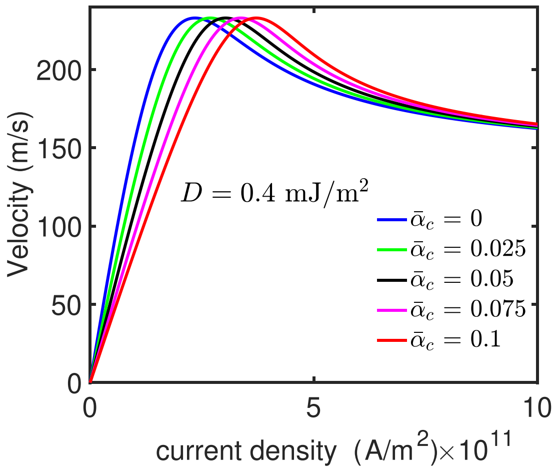

FIG. 5. The dependence of DW velocity on the current density in the presence of DMI driven by spin-orbit torque for various CD strengths. (a) An increase in the strength of CD and thus the effective damping leads to an increase in the $j_e^{\rm WB}$ but does not alter $v_{\rm max}^{\rm WB}$. Above the WB, the DMI induces a finite DW tilt ϕ, resulting in both CD and spin-orbit torque remaining finite and consequently producing a nonzero DW velocity.

access to the material parameters such as $\Lambda_{\rm R}$ and $\chi_{\rm R}^{\rm cd}$. By coherently incorporating both the DMI and CD, we achieved analogous results to the spin-transfer torque case, as illustrated in Fig. 3(c). Here, we observe an enhancement in $j_e^{\rm WB}$ attributable to a combination of DMI and CD, whereas an enhancement in $v_{\rm max}^{\rm WB}$ is predominantly driven by the DMI. An argument advocating for the coexistence of CD and the DMI is warranted, even though their relative strengths are likely to be strongly influenced by the precise crystallographic structure. This raises concerns about the validity of our calculations presented in Fig. 3(b) (see also blue curves in Fig. 4), where we neglected the DMI ($D = 0$). Therefore, we conducted further simulations considering nonzero DMI, as depicted in Fig. 5. This approach is supported by the understanding that in metallic systems, damping is mediated by conduction electrons, which can inherit tunable induced chirality due to inherent inhomogeneities in real materials and Hund's rule coupling. As illustrated in Fig. 5, our findings indicate that even in the presence of DMI, CD does not affect $v_{\rm max}^{\rm WB}$. Additionally, it is noteworthy that distinguishing between DMI and CD is possible by artificially adjusting the tilt angle. This adjustment can be achieved using an external in-plane field, allowing for a switch between different chiralities. By doing so, one can analyze how the current-driven velocity slope alters in the presence of either DMI alone or CD alone, as outlined in Ref. [8].

V. DISCUSSION AND CONCLUSIONS

We employ simple heuristic arguments guided by recent microscopic theories to suggest that CD can be expressed in terms of Lifshitz invariants, similar to the energy density for the DMI. This formulation offers a clearer foundation for integrating CD into current and field-driven dynamics of chiral magnetic DWs, and, by extension, into other exotic magnetic textures such as skyrmions, hopfions, and antiferromagnets. Our findings have been presented under the understanding that a reduction in the magnetic energy density induced by DMI would correspond to an overall increase in damping (i.e., a positive value for $\bar{\alpha}_c$), as suggested by Eqs. (3) and (4), and supported by previous studies [31–33]. However, as discussed earlier, this does not preclude the possibility of inhomogeneity-induced anisotropic effects that are prevalent in real materials. Such effects could lead to an overall reduction in damping (i.e., a negative value for $\bar{\alpha}_c$ while still maintaining overall positive damping). This scenario would be particularly intriguing in higher-dimensional magnetic textures, where such an anisotropy could result in directional variations in effective damping across different crystallographic directions. Additionally, since the dynamics of conduction electrons and magnetization occur at different timescales, in two-sublattice antiferromagnetic systems, such anisotropy could result in sublattice-dependent tunable chiral contributions to damping. As a matter of fact, investigations on Gilbert damping and spin pumping in two-sublattice magnets [13–15] indicate that the damping across sublattices can facilitate such an asymmetry. It is anticipated that differences in effective damping between the two sublattices could lead to asymmetry, thereby generating an additional drag force that may affect the dynamics of magnetic textures, particularly those strongly bound by robust antiferromagnetic exchange interactions.

In summary, we revisited the nature and effects of CD and the DMI in chiral ferromagnetic nanowires with broken inversion symmetry. We found that CD, like DMI, can be described in terms of Lifshitz invariants derived from the system's symmetry. This formulation facilitates the integration of CD into the dynamics of various chiral magnetic textures. Through theoretical analysis, we explored the impact of CD on current-induced motion of chiral DWs driven by spin-transfer torque and the spin Hall effect. We demonstrated the ability to distinguish CD's influence from that of DMI by studying current-induced dynamics. Specifically, below the WB, DMI does not affect DW velocity, whereas increased CD strength decreases DW velocity. Moreover, for spin-orbit torque-driven motion, DMI enhances both the $j_e^{\rm WB}$ and $v_{\rm max}^{\rm WB}$, whereas CD only enhances $j_e^{\rm WB}$ without affecting $v_{\rm max}^{\rm WB}$. It is important to highlight that, within Thiele's formalism as described, the impact of an out-of-plane external magnetic field H_z on DW dynamics is very similar to the effect of nonadiabatic spin-transfer torque. Consequently, H_z is anticipated to yield comparable results without introducing any novel physics. These findings present exciting prospects for exploration in exotic magnetic textures, offering opportunities for experimental validation and further understanding of their dynamics.

ACKNOWLEDGMENTS

C.A.A. expresses gratitude to Mu-Kun Lee and Oleg Tretiakov for insightful discussions. C.A.A. and M.M. acknowledge support from CREST, Japan Science and Technology Agency (Grant No. JPMJCR20T1). M.M. also acknowledges support from JSPS KAKENHI (Grants No. 20H00337, No. 23H04522, and No. 24H02231), and the Waseda University

Grant for Special Research Projects (Grants No. 2023C-140 and No. 2024C-153). G.T. and C.A.A. acknowledge support from a Grant-in-Aid for Scientific Research (B) (No. 21H01034) from the Japan Society for the Promotion of Science. A.M. was supported by Grant ANR-23-CE09-0034-03 "NEXT" of the French Agence Nationale de la Recherche.

[1] A. N. Bogdanov and U. K. Rößler, Chiral symmetry breaking in magnetic thin films and multilayers, Phys. Rev. Lett. **87**, 037203 (2001).

[2] I. E. Dzyaloshinskii, Theory of helicoidal structures in antiferromagnets. I. Nonmetals, Sov. Phys. JETP **19**, 960 (1964).

[3] I. Dzyaloshinsky, A thermodynamic theory of "weak" ferromagnetism of antiferromagnetics, J. Phys. Chem. Solids **4**, 241 (1958).

[4] T. Moriya, Anisotropic superexchange interaction and weak ferromagnetism, Phys. Rev. **120**, 91 (1960).

[5] A. Fert and P. M. Levy, Role of anisotropic exchange interactions in determining the properties of spin-glasses, Phys. Rev. Lett. **44**, 1538 (1980).

[6] E. Jué, C. K. Safeer, M. Drouard, A. Lopez, P. Balint, L. Buda-Prejbeanu, O. Boulle, S. Auffret, A. Schuhl, A. Manchon, I. M. Miron, and G. Gaudin, Chiral damping of magnetic domain walls, Nat. Mater. **15**, 272 (2016).

[7] A. Ganguly, S. Zhang, Senfu, I. M. Miron, I. Mihai, J. Kosel, X. Zhang, A. Manchon, N. Singh, D. H. Anjum, and G. Das, Competition between chiral energy and chiral damping in the asymmetric expansion of magnetic bubbles, ACS Appl. Electron. Mater. **3**, 4734 (2021).

[8] C. K. Safeer, M.-A. Nsibi, J. Nath, M. S. Gabor, H. Yang, I. Joumard, S. Auffret, G. Gaudin, and I. M. Miron, Effect of chiral damping on the dynamics of chiral domain walls and skyrmions, Nat. Commun. **13**, 1192 (2022).

[9] C. A. Akosa, I. M. Miron, G. Gaudin, and A. Manchon, Phenomenology of chiral damping in noncentrosymmetric magnets, Phys. Rev. B **93**, 214429 (2016).

[10] F. Freimuth, S. Blügel, and Y. Mokrousov, Chiral damping, chiral gyromagnetism, and current-induced torques in textured one-dimensional Rashba ferromagnets, Phys. Rev. B **96**, 104418 (2017).

[11] K.-W. Kim, H.-W. Lee, K.-J. Lee, K. Everschor-Sitte, O. Gomonary, and J. Sinova, Roles of chiral renormalization on magnetization dynamics in chiral magnets, Phys. Rev. B **97**, 100402(R) (2018).

[12] C. A. Akosa, A. Takeuchi, Z. Yuan, and G. Tatara, Theory of chiral effects in magnetic textures with spin-orbit coupling, Phys. Rev. B **98**, 184424 (2018).

[13] A. Kamra and W. Belzig, Spin pumping and shot noise in ferrimagnets: Bridging ferro- and antiferromagnets, Phys. Rev. Lett. **119**, 197201 (2017).

[14] Q. Liu, H. Y. Yuan, K. Xia, and Z. Yuan, Mode-dependent damping in metallic antiferromagnets due to intersublattice spin pumping, Phys. Rev. Mater. **1**, 061401(R) (2017).

[15] A. Kamra, R. E. Troncoso, W. Belzig, and A. Brataas, Gilbert damping phenomenology for two-sublattice magnets, Phys. Rev. B **98**, 184402 (2018).

[16] K.-W. Kim, H.-W. Lee, K.-J. Lee, and M. D. Stiles, Chirality from interfacial spin-orbit coupling effects in magnetic bilayers, Phys. Rev. Lett. **111**, 216601 (2013).

[17] A. Kundu and S. Zhang, Dzyaloshinskii-Moriya interaction mediated by spin-polarized band with Rashba spin-orbit coupling, Phys. Rev. B **92**, 094434 (2015).

[18] T. Kikuchi, T. Koretsune, R. Arita, and G. Tatara, Dzyaloshinskii-Moriya interaction as a consequence of a Doppler shift due to spin-orbit-induced intrinsic spin current, Phys. Rev. Lett. **116**, 247201 (2016).

[19] K. Yamamoto, A.-M. Pradipto, K. Nawa, T. Akiyama, T. Ito, T. Ono, and K. Nakamura, Interfacial Dzyaloshinskii-Moriya interaction and orbital magnetic moments of metallic multilayer films, AIP Adv. **7**, 056302 (2017).

[20] K. M. D. Hals and A. Brataas, Spin-orbit torques and anisotropic magnetization damping in skyrmion crystals, Phys. Rev. B **89**, 064426 (2014).

[21] R. C. Powell, *Symmetry, Group Theory and the Physical Properties of Crystals* (Springer, New York, 2010).

[22] J.-V. Kim, Role of nonlinear anisotropic damping in the magnetization dynamics of topological solitons, Phys. Rev. B **92**, 014418 (2015).

[23] S. Brinker, M. D. S. Dias, and S. Lounis, Generalization of the Landau–Lifshitz–Gilbert equation, by multi-body contributions to Gilbert damping for non-collinear magnets, J. Phys.: Condens. Matter **34**, 285802 (2022).

[24] G. Dresselhaus, Spin-orbit coupling effects in zinc blende structures, Phys. Rev. **100**, 580 (1955).

[25] Y. A. Bychkov and E. I. Rashba, Properties of a 2D electron gas with lifted spectral degeneracy, JETP Lett. **39**, 78 (1984).

[26] R. Mondal, M. Berritta, and P. M. Oppeneer, Relativistic theory of spin relaxation mechanisms in the Landau-Lifshitz-Gilbert equation of spin dynamics, Phys. Rev. B **94**, 144419 (2016).

[27] R. Mondal, M. Berritta, A. K. Nandy, and P. M. Oppeneer, Relativistic theory of magnetic inertia in ultrafast spin dynamics, Phys. Rev. B **96**, 024425 (2017).

[28] A. D. Caviglia, M. Gabay, S. Gariglio, N. Reyren, C. Cancellieri, and J.-M. Triscone, Tunable Rashba spin-orbit interaction at oxide interfaces, Phys. Rev. Lett. **104**, 126803 (2010).

[29] Y. H. Park, H.-J. Kim, J. Chang, S. H. Han, J. Eom, H.-J. Choi, and H. C. Koo, Separation of Rashba and Dresselhaus spin-orbit interactions using crystal direction dependent transport measurements, Appl. Phys. Lett. **103**, 252407 (2013).

[30] C. Ciccarelli, L. Anderson, V. Tshitoyan, A. J. Ferguson, F. Gerhard, C. Gould, L. W. Molenkamp, J. Gayles, J. Železný, L. Šmejkal, Z. Yuan, J. Sinova, F. Freimuth, and T. Jungwirth, Room-temperature spin-orbit torque in NiMnSb, Nat. Phys. **12**, 855 (2016).

[31] P. M. Levy and S. Zhang, Resistivity due to domain wall scattering, Phys. Rev. Lett. **79**, 5110 (1997).

[32] Z. Yuan, Y. Liu, A. A. Starikov, P. J. Kelly, and A. Brataas, Spin-orbit-coupling-induced domain-wall resistance in diffusive ferromagnets, Phys. Rev. Lett. **109**, 267201 (2012).

[33] C. A. Akosa, W.-S. Kim, A. Bisig, M. Kläui, K.-J. Lee, and A. Manchon, Role of spin diffusion in current-induced domain

wall motion for disordered ferromagnets, Phys. Rev. B **91**, 094411 (2015).
[34] V. Kamberský and C. E. Patton, Spin-wave relaxation and phenomenological damping in ferromagnetic resonance, Phys. Rev. B **11**, 2668 (1975).
[35] V. Kamberský, On ferromagnetic resonance damping in metals, Czech. J. Phys. B **26**, 1366 (1976).
[36] V. Kamberský, FMR linewidth and disorder in metals, Czech. J. Phys. B **34**, 1111 (1984).
[37] A. Brataas, Y. Tserkovnyak, and G. E. W. Bauer, Scattering theory of Gilbert damping, Phys. Rev. Lett. **101**, 037207 (2008).
[38] Y. Liu, A. A. Starikov, Z. Yuan, and P. J. Kelly, First-principles calculations of magnetization relaxation in pure Fe, Co, and Ni with frozen thermal lattice disorder, Phys. Rev. B **84**, 014412 (2011).
[39] A. A. Thiele, Steady-state motion of magnetic domains, Phys. Rev. Lett. **30**, 230 (1973).
[40] O. Boulle, L. D. Buda-Prejbeanu, M. Miron, and G. Gaudin, Current induced domain wall dynamics in the presence of a transverse magnetic field in out-of-plane magnetized materials, J. Appl. Phys. **112**, 053901 (2012).
[41] O. Boulle, L. D. Buda-Prejbeanu, E. Jué, I. M. Miron, and G. Gaudin, Current induced domain wall dynamics in the presence of spin orbit torques, J. Appl. Phys. **115**, 17D502 (2014).
[42] N. L. Schryer and L. R. Walker, The motion of 180° domain walls in uniform dc magnetic fields, J. Appl. Phys. **45**, 5406 (1974).
[43] C. A. Akosa, H. Li, G. Tatara, and O. A. Tretiakov, Tuning the skyrmion Hall effect via engineering of spin-orbit interaction, Phys. Rev. Appl. **12**, 054032 (2019).
[44] A. Mougin, M. Cormier, J. P. Adam, J. Metaxas, and J. Ferré, Domain wall mobility, stability and Walker breakdown in magnetic nanowires, Europhys. Lett. **78**, 57007 (2007).
[45] P. J. Metaxas, J. P. Jamet, A. Mougin, M. Cormier, J. Ferré, V. Baltz, B. Rodmacq, B. Dieny, and R. L. Stamps, Creep and flow regimes of magnetic domain-wall motion in ultrathin Pt/Co/Pt films with perpendicular anisotropy, Phys. Rev. Lett. **99**, 217208 (2007).
[46] A. Thiaville, S. Rohart, É. Jué, V. Cros and A. Fert, Dynamics of Dzyaloshinskii domain walls in ultrathin magnetic films, Europhys. Lett. **100**, 57002 (2012).
[47] S. Emori, U. Bauer, S. Woo, and G. S. D. Beach, Large voltage-induced modification of spin-orbit torques in Pt/Co/GdOx, Appl. Phys. Lett. **105**, 222401 (2014).
[48] E. Lesne, Y. Fu, S. Oyarzun, J. Rojas-Sánchez, D. Vaz, H. Naganuma, G. Sicoli, J.-P. Attané, M. Jamet, E. Jacquet, J.-M. George, A. Barthélémy, H. Jaffrès, A. Fert, M. Bibes, and L. Vila, Highly efficient and tunable spin-to-charge conversion through Rashba coupling at oxide interfaces, Nat. Mater. **15**, 1261 (2016).
[49] C. Yin, P. Seiler, L. M. K. Tang, I. Leermakers, N. Lebedev, U. Zeitler, and J. Aarts, Tuning Rashba spin-orbit coupling at $LaAlO_3/SrTiO_3$ interfaces by band filling, Phys. Rev. B **101**, 245114 (2020).